2

Applied Research Laboratory

Technical Report

FLAT PLAT VIBRATION ANALYSIS
EXPERIMENTAL AND NUMERICAL
FILLET STUDY

by

R.D. Cook
D.E. Thompson

PENNSTATE

1855

2

The Pennsylvania State University
APPLIED RESEARCH LABORATORY
P.O. Box 30
State College, PA 16804

FLAT PLAT VIBRATION ANALYSIS EXPERIMENTAL AND NUMERICAL FILLET STUDY

by

R.D. Cook
D.E. Thompson

Technical Report No. TR 90-001
February 1990

Supported by:
Space and Naval Warfare Systems Command

L.R. Hettche, Director
Applied Research Laboratory

Approved for public release; distribution unlimited

UNCLASSIFIED

SECURITY CLASSIFICATION OF THIS PAGE

REPORT DOCUMENTATION PAGE

1a. REPORT SECURITY CLASSIFICATION Unclassified	1b. RESTRICTIVE MARKINGS
2a. SECURITY CLASSIFICATION AUTHORITY 2b. DECLASSIFICATION / DOWNGRADING SCHEDULE	3. DISTRIBUTION / AVAILABILITY OF REPORT Approved for public release; distribution unlimited.
4. PERFORMING ORGANIZATION REPORT NUMBER(S) TR- 90-01	5. MONITORING ORGANIZATION REPORT NUMBER(S) N00039-88-C-0051
6a. NAME OF PERFORMING ORGANIZATION Applied Research Laboratory Penn State University 6b. OFFICE SYMBOL (If applicable) ARL	7a. NAME OF MONITORING ORGANIZATION DARPA Naval Technology Office
6c. ADDRESS (City, State, and ZIP Code) P.O. Box 30 State College, PA 16804	7b. ADDRESS (City, State, and ZIP Code) 1400 Wilson Blvd. Arlington, VA 22209-2308
8a. NAME OF FUNDING / SPONSORING ORGANIZATION Space and Naval Warfare Systems Command 8b. OFFICE SYMBOL (If applicable) SPAWAR	9. PROCUREMENT INSTRUMENT IDENTIFICATION NUMBER
8c. ADDRESS (City, State, and ZIP Code) Department of the Navy Washington, DC 20363-5100	10. SOURCE OF FUNDING NUMBERS PROGRAM ELEMENT NO. / PROJECT NO. / TASK NO. / WORK UNIT ACCESSION NO.

11. TITLE (Include Security Classification)
Flat Plat Vibration Analysis Experimental and Numerical Fillet Study

12. PERSONAL AUTHOR(S)
R. D. Cook and D. E. Thompson

13a. TYPE OF REPORT	13b. TIME COVERED	14. DATE OF REPORT (Year, Month, Day)	15. PAGE COUNT
Final	FROM ______ TO ______	February 1990	51

16. SUPPLEMENTARY NOTATION

17. COSATI CODES		
FIELD	GROUP	SUB-GROUP

18. SUBJECT TERMS (Continue on reverse if necessary and identify by block number)
plates; resonance; mode shape; laser vibrometer; NASTRAN; water loading

19. ABSTRACT (Continue on reverse if necessary and identify by block number)

Measurements and predictions of low-order resonant frequencies and mode shapes have been made for three rectangular aluminum plates, each having a different fillet radius at the attached end. Measurements were conducted using a dual-beam laser vibrometer, and predictions were made using the MSC/NASTRAN finite element code. The effects of the fillet radius on the resonant frequencies have been quantified, and a comparison between measured and predicted values is presented. Effects of water loading are also presented. Results show that 1) resonant frequencies increase as the filet radius increases, 2) the predicted resonant frequencies compare favorably with those measured, and 3) water loading reduces the resonant frequencies determined in air.

20. DISTRIBUTION / AVAILABILITY OF ABSTRACT ☒ UNCLASSIFIED/UNLIMITED ☐ SAME AS RPT. ☐ DTIC USERS	21. ABSTRACT SECURITY CLASSIFICATION Unclassified
22a. NAME OF RESPONSIBLE INDIVIDUAL D. E. Thompson	22b. TELEPHONE (Include Area Code) 814/865-1741 22c. OFFICE SYMBOL ARL

DD FORM 1473, 84 MAR

83 APR edition may be used until exhausted.
All other editions are obsolete.

SECURITY CLASSIFICATION OF THIS PAGE

UNCLASSIFIED

Abstract

Measurements and predictions of low-order resonant frequencies and mode shapes have been made for three rectangular aluminum plates, each having a different fillet radius at the attached end. Measurements were conducted using a dual-beam laser vibrometer, and predictions were made using the MSC/NASTRAN finite element code. The effects of the fillet radius on the resonant frequencies have been quantified, and a comparison between measured and predicted values is presented. Effects of water loading are also presented. Results show that 1) resonant frequencies increase as the fillet radius increases, 2) the predicted resonant frequencies compare favorably with those measured, and 3) water loading reduces the resonant frequencies determined in air.

Table of Contents

Acknowledgements

The author wishes to express his gratitude to Dr. Donald E. Thompson for his guidance and support also the numerical modeling expertise of Mr. John T. Pitterle is appreciated. This work was supported by DARPA Naval Technology Office.

List of Tables

List of Figures

List of Figures (continued)

Chapter 1

Introduction and Scope of Investigation

Plate-like structures have use in many applications. Their strength and dynamic response play a key role in determining their efficient behavior. A knowledge of the relationship between physical properties of a structure and its modal parameters can provide considerable insight into the method for lessening the effects of undesirable structural responses. Because the vibrational response of a plate-like structure can depend on various parameters, we need to quantify the effects of parameter variations on vibrational response.

This quantitative study investigates the effects of boundary conditions on the dynamic response of rectangular plate-like structures with one edge attached. The fillet radius at the attached edge will be varied and measurements made with and without endplates adjoining the attachment base. These systematic changes of the boundary conditions at the attached edge will be made and the effect on the modal parameters, resonant frequencies and mode shapes determined. Experimental and numerical (MSC/NASTRAN) finite element results will be obtained for plates in air and water. This investigation will 1) quantify the effects that certain boundary conditions have on the dynamic response of plates, 2) validate the numerical modeling capability of MSC-NASTRAN to predict the resonant responses of plates with fillets in air and water, and 3) determine fluid-loading effects on the modal parameters for attached plates.

Chapter 2

Experimental Investigation

2.1 Experimental Approach

A one-piece flat rectangular plate with a perpendicular end-plate (base) was machined from a block of (6061T6) aluminum. A radius was machined at the intersection of the plate and base, Figure 1. Tests were conducted with and without the adjoining end plates attached to the baseplate and support block. For each test, the baseplate was rigidly bolted to a 12 inch x 13.5 inch x 1.75 inch aluminum block. The ratio of the mass of the plate to the mass of the support was approximately one. Excitation of the plate was by means of a small speaker for measurements in air and by a J9 hydrophone for measurements in water. The speaker and hydrophone were driven by a sine signal generator which was automatically swept across the frequency range of interest. The low order resonant frequencies and mode shapes were measured using a scanning dual-beam laser vibrometer system, Reference [1-3]. Fluid loading effects were also examined by comparing experimental results obtained in air and water. This set of experimental measurements was made for three different machined fillet radii, R = 0.5, 0.75 and 1.5 inches. The ratio of the fillet radius to plate thickness was 0.33, 0.5 and 1.0 for the 0.5, 0.75 and 1.5 inch radii, respectively.

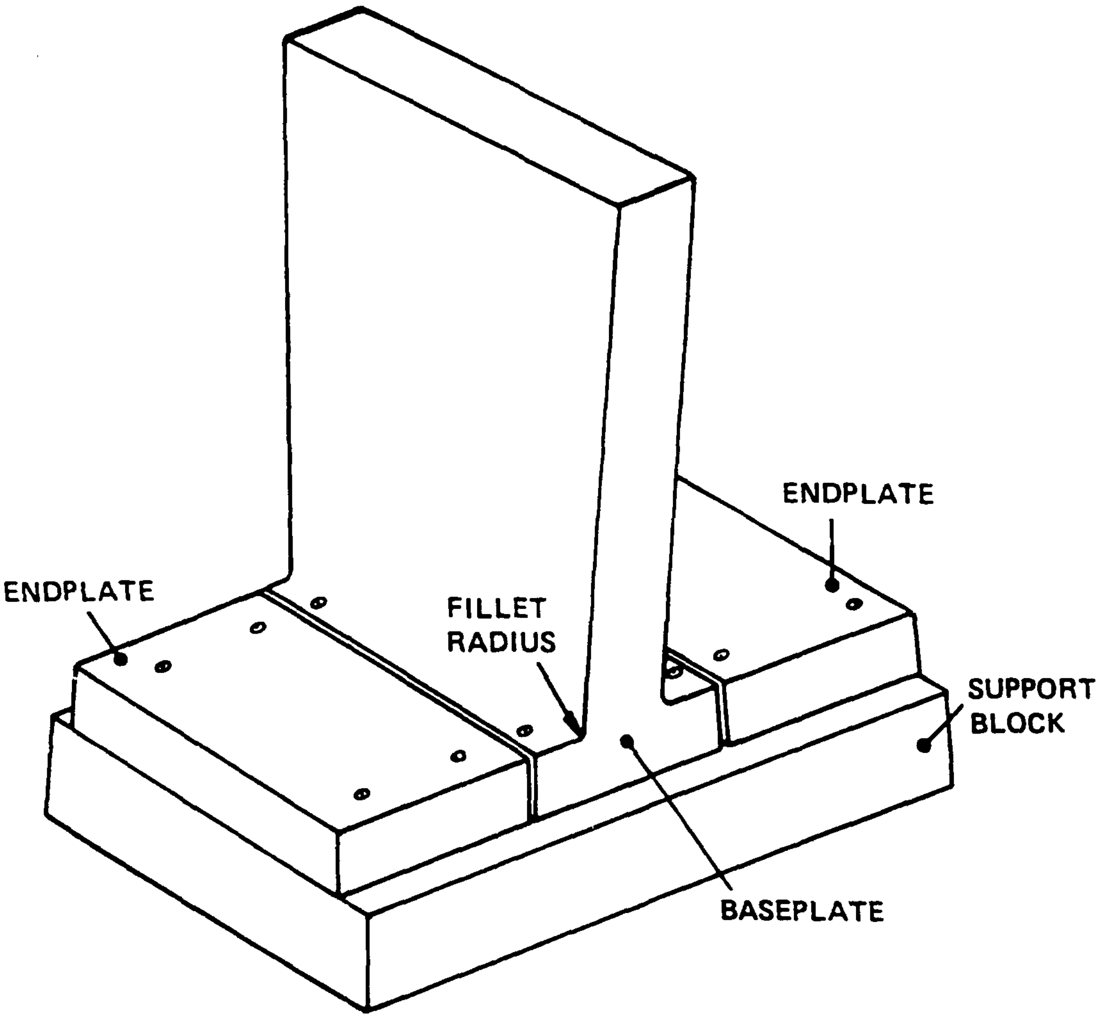

Figure 1. Plate Arrangement

2.2 Instrumentation

A sinusoidal acoustic source was used as the vibration exciter. This method has the advantage of no local mass loading and the area of force application is considered to be small compared to the wavelength of the highest resonant frequency measured. A block diagram of the acoustic vibrational driving instrumentation is shown in Figure 2. A frequency sweep oscillator, along with a small speaker for in air measurements and a J9 hydrophone for in water measurements, driven by a power amplifier was used as the vibration source. The source input voltage was measured by an RMS voltage meter.

The dual-beam laser vibrometer was used as the plate vibration measurement system in this study. This noncontact vibration measuring device has the advantage of excellent mobility, i.e., a series of measurements can be taken at many points on the structure, and no effects of mass loading of the structure would be present. A block diagram of the vibration measurement instrumentation is shown in Figure 3. A 4-watt Lexel Argon-Ion laser and its associated optics is positioned on a Newport Research Series optical bench with nitrogen filled isolation legs. This scanning dual-beam laser vibrometer system was set up in its reference-beam mode which measures local normal velocities at the surface of vibrating objects. The laser vibrometer operation is based on the Doppler shift of laser light scattered by a vibrating surface. A pre-shifted beam, the reference beam, is mixed with the backscattered light from the vibrating surface and collected onto the surface of a photodetector. Movement of the vibrating surface

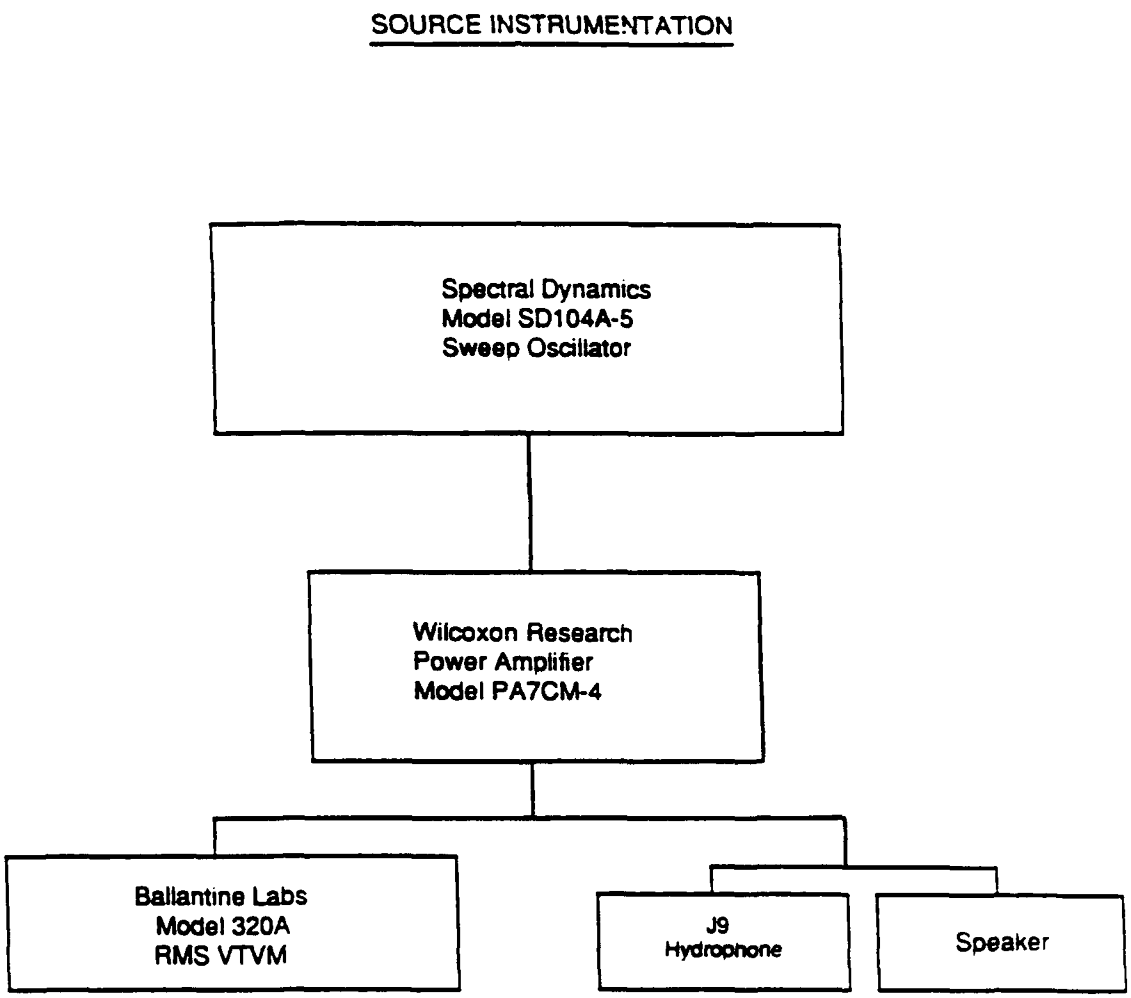

Figure 2. Block Diagram of the Acoustic Vibrational Driving Instrumentation

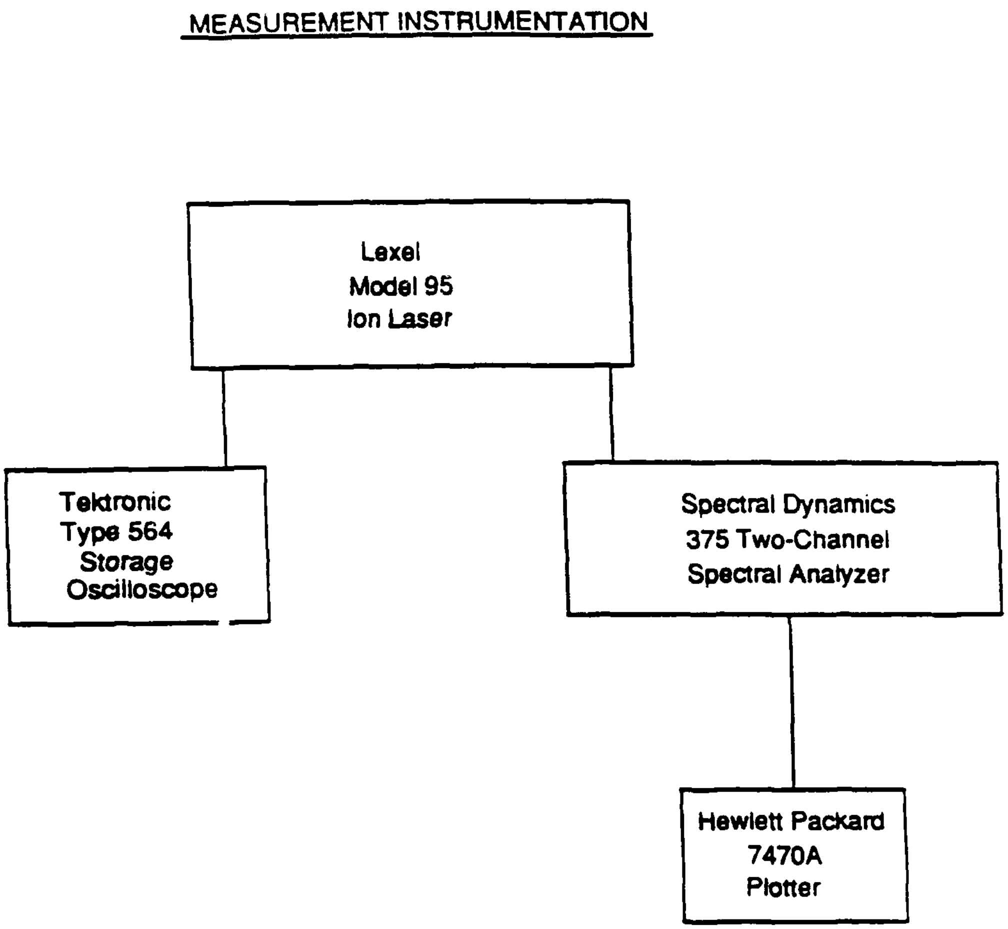

Figure 3. Block Diagram of the Vibration Measurement Instrumentation

produoes a Doppler frequency shift in the backscattered light which is heterodyned with that from the reference beam into the photodetector. Photodetector current is modulated at this Doppler frequency which is proportional to the surface velocity of the vibrating object. An FM demodulator processes the photodetector current to give a real-time analogue representation of surface-normal velocity. For further details on the operating description of the dual-beam laser vibrometer system, refer to Reference [1-3].

2.3 Test Procedure and Conditions for Vibration Measurements

All tests were performed in the Optics Laboratory at the Garfield Thomas Water Tunnel building of ARL Penn State. The specimens used in this investigation consisted of three 10 x 17.5 x 1.5 inch rectangular aluminum (6061T6) plates each having a 10 x 4.5 x 1 inch rectangular aluminum base plate. Fillet radii machined between the plate and the base plate were 0.5, 0.75 and 1.5 inches. In addition, two 10 x 4.5 x 1 inch rectangular aluminum plates were made to be used as the end plates adjoining the attachment base. A typical plate arrangement is shown in Figure 1. The plates were placed in a 6 x 2.5 x 2.5 foot tank having 1/2 inch thick plexiglass walls. The plates were positioned to one end of the tank where the tank window vibrations due to the acoustic source input was minimum compared to the vibration levels of the plate. This would ensure minimum distortion effects due to window vibration. To minimize the vibrations due to the environment, the tank was placed on a granite block table supported by rubber isolation mounts. The position of the plates in the tank and the water level was noted and maintained constant for all tests since this consistency would ensure the repeatability of testing conditions and guarantee similar loading conditions for all plates tested in water.

For each plate tested, the vibrational response was measured. For these investigations, sinusoidal excitation was applied at one of the upper corners of the plate. This point was used rather than a point on one of the axes of symmetry in order to excite several kinds of modes, rather than only those with a particular symmetry. The plate response measurement was located at one of the upper corners, opposite the drive location. For the low-order modes, this location has maximum deflection amplitudes.

The frequency sweep rate was set to sweep automatically. From the resulting plots of amplitude vs. frequency, the identification of several low-order resonant frequencies was made by looking for peaks in the response spectrum. It was not determined whether the exciting force was flat with frequency over the range of interest, therefore in order to identify plate resonant frequencies, mode shapes for the observed peaks were measured and identified. At these low frequencies, the modal density in the plate is low and the resonance peaks were well separated.

In order to accurately determine the order of a particular normal mode of vibration, mapping the displacement amplitude over the plate surface and measuring the relative phase values was required. The scanning capability of the dual-beam laser vibrometer was utilized for these measurements across the surface of the plate in two dimensions. For each resonant frequency measured, the mode shape was determined by first sinusoidally exciting the plate at the resonant frequency of interest and then scanning the surface of the plate to determine the phase and amplitude at each measurement point. One of the beams from the dual-beam laser vibrometer was used as a reference, while the second beam was used to scan the plate surface. The reference beam was located at one of the upper corners of the plate. For the scanning beam, measurement locations were marked with reflective paint. A grid of points one inch from the top and side plate edges and spaced every two inches along the length and width was laid out. Near the bottom of the plate in the fillet region, measurement points were spaced one inch apart along the length of the plate spanning three rows, Figure 4. Phase and amplitude information were obtained for all of these measurement points. At a given resonant frequency when a structure is lightly damped, it will exhibit normal modes of vibration. This is characterized by the fact that all points of the structure are moving either in phase (0 degrees) or out of phase (180 degrees) with respect to a reference phase and depend only on the shape of the normal mode. An example of a mode shape measurement is shown in Figure 4. The boundary between the measured 0 degree and 180 degree phases defines the nodal lines for the mode. Amplitude measurements helped to identify the nodal lines but are not shown in the illustration.

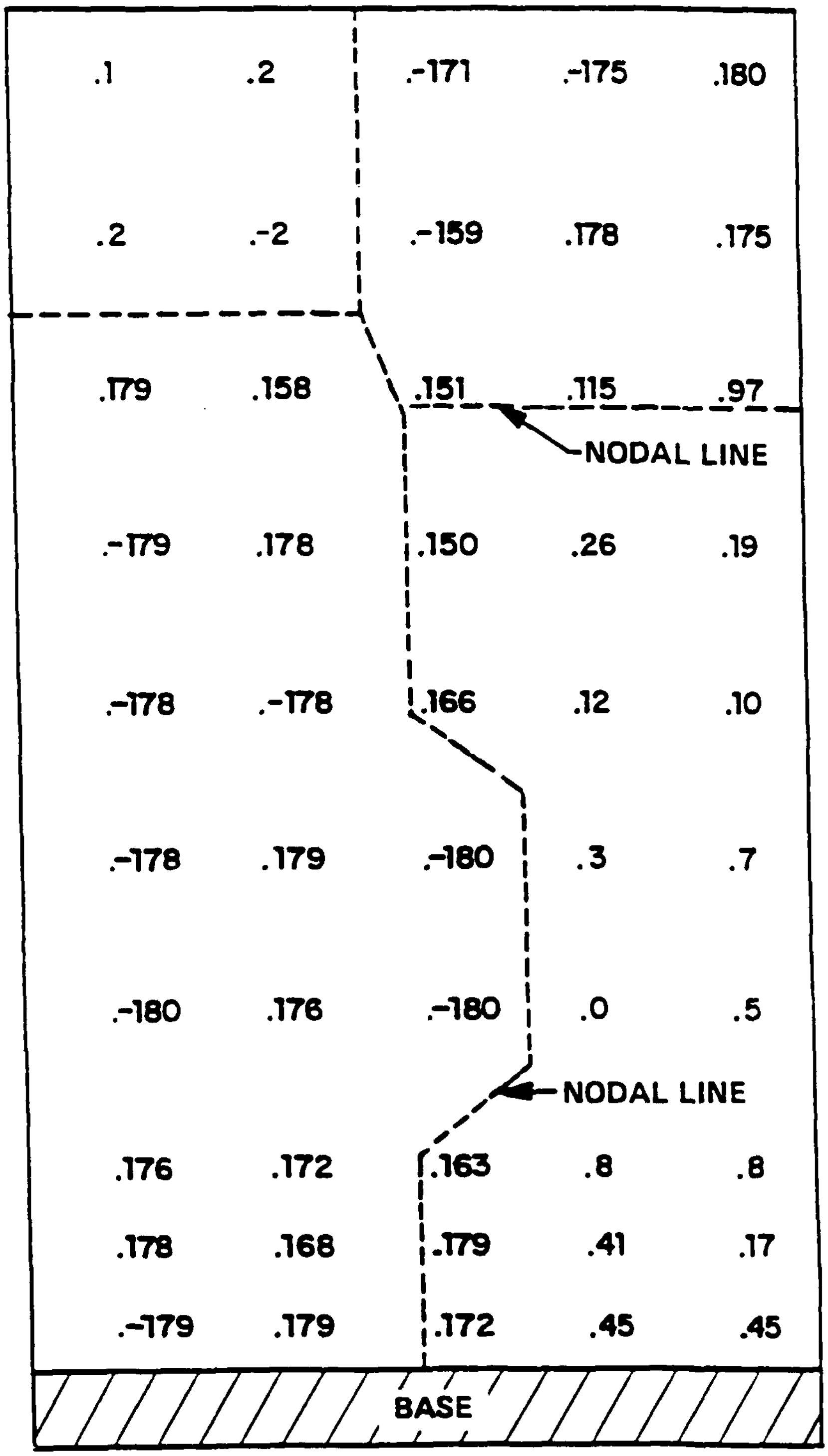

Figure 4. Example of Mode Shape Measurement where Phases of Vibration are Measured Relative to Drive Point at Upper Left Hand Corner

2.4 Data Acquisition

The real-time output signals of the laser vibrometer were converted to a frequency spectrum by a Fast Fourier Transform (FFT) performed on the Spectral Dynamics SD375 Analyzer. Amplitude vs. frequency spectra were generated using the peak averaging mode. The bandwidth of the spectra for a 0-2 kHZ frequency range was 5 HZ. Resonant frequencies with 0.25 HZ resolution were observed using the frequency zoom capability of the SD375. Real-time output signal-to-noise was monitored using the Tektronic Oscilloscope.

Chapter 3

Numerical Modeling

3.1 NASTRAN Model Description

The resonant frequencies and mode shapes of the plate with fillet radii of 0.5, 0.75 and 1.5 inches were predicted using the MSC/NASTRAN finite element code, Reference [4]. Three-dimensional solid elements were used in all the predictions because of the three-dimensional character of this particular structure. Predictions for the resonances of the plates in water were made using the fluid-loading option in NASTRAN which generates mass and stiffness matrices that represent the properties of the fluid.

The entire finite element model consisted of the plate with fillet, support base plate and endplates which were all modeled using eight node solid elements (HEXA). All bolt connections were modeled using rigid body elements (RBE). In the critical area of the plate, the fillet region, the element size was small, whereas in more distant regions larger elements were used, Figure 5. The average height of a element used in the fillet region was one sixth of the fillet radius for each radii investigated. The elements used for the fillet were not curved, but this refinement was sufficient to produce a constant radius fillet segment. Two numerical models were investigated in order to determine how the boundary condition would be described. The first model consisted of the support and the base of the plate sharing common grid points only at the bolt locations. In this model relative motion

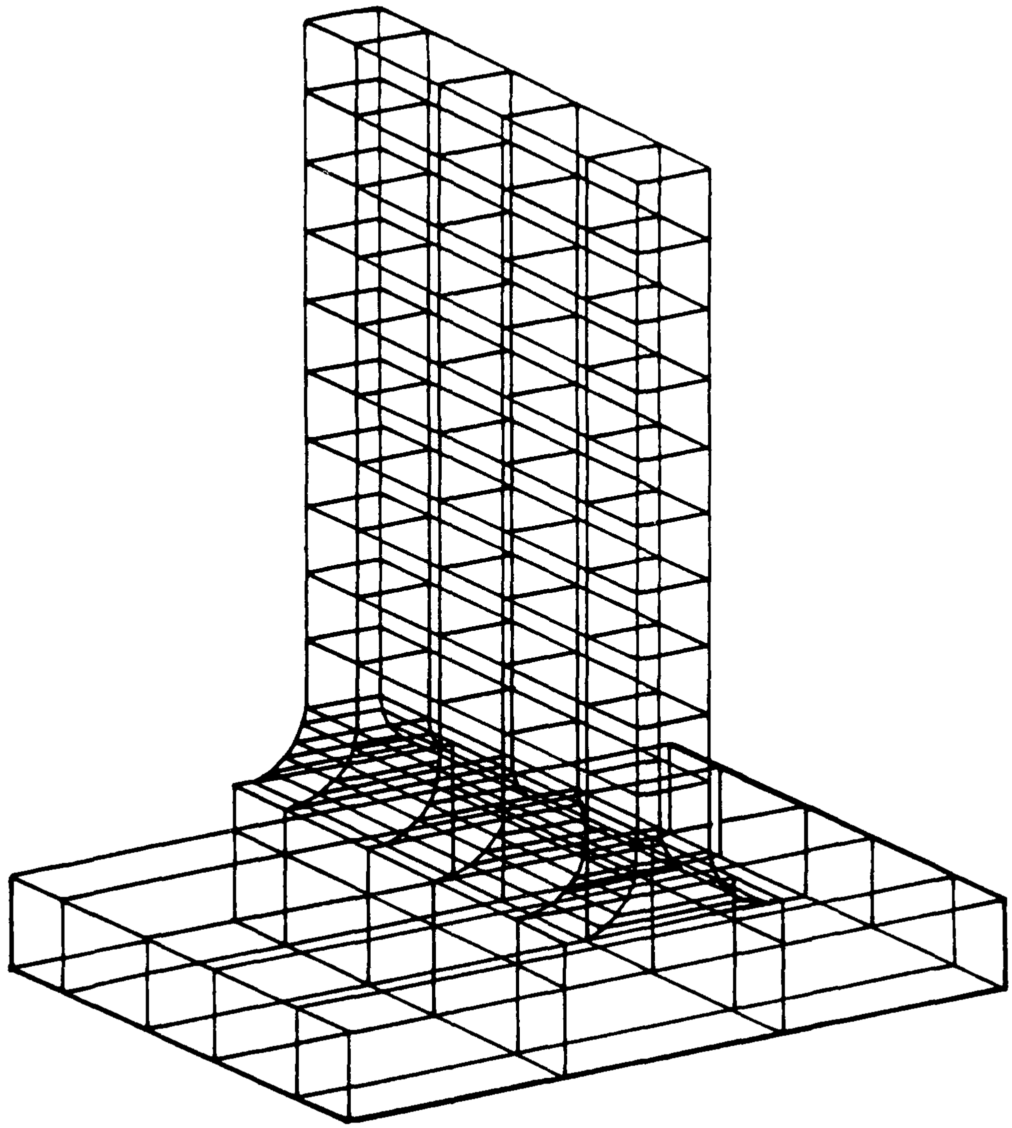

Figure 5. Finite Element Model Arrangement

between the two structures could occur. The second model consisted of the support and the base of the plate sharing common grid points entirely, therefore no relative motion between the two structures could occur. Resonant frequencies obtained for both models were compared to measured values. The first model, plate attached to support only at bolt locations, produced values for the modes which were high compared to measured values. The second model, plate attached to support entirely, produced values for the modes which were closer to the measured values. Based on these results, the second model was chosen for this study. Also in the program, the motion at the grid points along the bottom of the support were suppressed entirely. Figure 5 shows the element arrangement of support and plate for the case of fillet radius equal 1.5 inches. The same modeling scheme was applied to all the plates analyzed.

Chapter 4

Discussion of Results

4.1 Repeatability of Results

The repeatability of the measured resonant frequencies based on two independent measurements are shown in Table 1. The first measurement is taken as the reference. With the exception of one frequency, the 0.5 inch fillet, the repeatability was better than ± 1.0 percent. The maximum of these percentage values versus mode of resonant frequency are presented in Figure 6 for air and water measurements independent of boundary conditions. For the repeat measurements, the plate was removed and repositioned so that the effects of the test setup could accurately be assessed. The worst agreement (repeatability) between two sets of measurements is shown in Figure 6 for measurements both in-air and in-water. No distinction is made of the plate boundary condition. This comparison shows that the level of repeatability appears to be mode and fluid medium dependent. A maximum percent repeatability occurs at the second bending mode of vibration for both air and water measurements. Also shown in Figure 6 is the fact that the repeatability in water measurements is improved by approximately a factor of three compared with those in air. An average spread of data is presented on subsequent plots of the measured resonant frequencies so any differences in the resonant frequencies as a function of fillet radius and other boundary conditions can be assessed in terms of the average spread in the measured data.

Table 1. Comparison of Repeat Resonant Frequency Measurements

Plate Fillet Radius	Test Condition	First Measurement	Second Measurement	Percent Difference
1.5 inch	Air-without endplates	605.75	605.5	0.04
		1824.5	1819.75	0.3
	Water - without endplates	484.75	483.75	0.2
		850.0	848.5	0.2
		1446.0	1443.0	0.2
	Air-with endplates	1831.0	1819.75	0.6
	Water-with endplates	810.0	806.25	0.5
		1357.0	1357.5	-0.04
0.75 inch	Air-without endplates	595.0	600.0	-0.8
		1078.0	1080.0	-0.2
		1808.5	1810.0	-0.08
	Water-without endplates	475.5	475.75	-0.05
		810.0	811.25	-0.15
		1413.0	1409.0	0.3
	Air-with endplates	586.6	590.0	-0.6
		1016.5	1020.0	-0.3
		1812.5	1820.0	-0.4
	Water-with endplates	464.25	463.75	0.1

(cont. on next page)

Table 1 (cont.)

Plate Fillet Radius	Test Condition	First Measurement	Second Measurement	Percent Difference
0.5 inch	Air-without endplates	584.875	585.75	-0.15
		1027.5	1012.0	1.5
		1775.5	1778.0	-0.14
	Water-without endplates	783.75	781.25	0.3
	Air-with endplates	576.75	578.0	-0.2
		998.5	1004.5	-0.6
		1789.0	1789.0	0

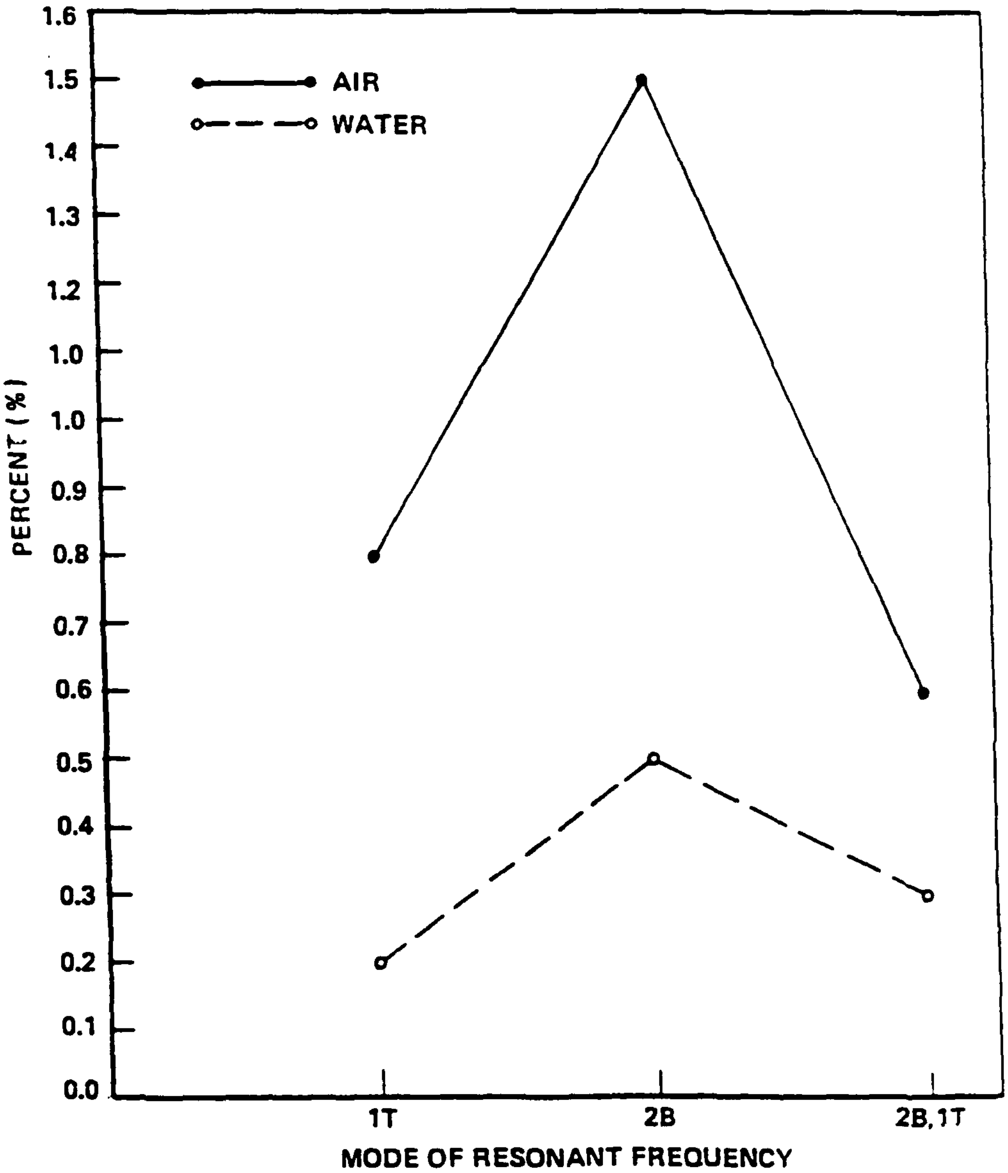

Figure 6. Maximum Difference Between Repeat Resonant Frequency Measurements as a Percent of Resonant Frequency for Plates in Air and Water

4.2 Resonant Frequencies

From the resonant frequency measurements presented in Table 1, average values were computed and used in all subsequent tables and figures. A comparison of the predicted and measured resonant frequencies for each mode of vibration is given in Table 2 through Table 5. The results in Table 2 and Table 3 are for the aluminum plates without the base endplates attached in air and water, respectively. The results in Table 4 and Table 5 are for the aluminum plates with the base endplates attached in air and water, respectively. The percent differences are also given in each table where negative percents indicate that the predicted resonant frequency is below the measured resonant frequency. The averages of the magnitude of the percent difference is 4.6 for the plates without base endplates in air and 9.6 for the plates without base endplates in water. For the plates with the base endplates, average percent difference is 2.9 for in air measurements and 9.6 for in water measurements. The maximum difference is 8.4 percent in-air and 17.5 percent in-water for plates without endplates attached and are 8.7 percent in-air and 12.6 percent in-water for plates with endplates attached. This information is shown in Table 6. The data show that most of the predicted values are lower than the measured values. The measured resonant frequencies compared favorably with those values predicted in air, but larger percent differences occurred for those values predicted in water.

Table 2. Comparison of Predicted and Measured Resonant Frequencies for Aluminum Plates without Base Endplates in Air

Plate Fillet Radius	Mode	Predicted Resonant Frequency	Measured Resonant Frequency	Percent Difference
1.5 inch	1T	603	606	-0.5
	2B	1054	1128	-6.6
	2B,1T	1976	1822	8.4
0.75 inch	1T	585	597	-2.0
	2B	1004	1079	-6.9
	2B,1T	1918	1809	6.0
0.5 inch	1T	580	585	-0.8
	2B	988	1020	-3.1
	2B,1T	1901	1777	7.0

Table 3. Comparison of Predicted and Measured Resonant Frequencies for Aluminum Plates without Base Endplates in Water

Plate Fillet Radius	Mode	Predicted Resonant Frequency	Measured Resonant Frequency	Percent Difference
1.5 inch	1T	449	484	-7.2
	2B	706	849	-16.8
	2B,1T	1514	1444	4.8
0.75 inch	1T	435	476	-8.6
	2B	669	811	-17.5
	2B,1T	1467	1411	3.9
0.5 inch	1T	431	466	-7.5
	2B	658	782	-15.8
	2B,1T	1454	1393	4.4

Table 4. Comparison of Predicted and Measured Resonant Frequencies for Aluminum Plates with Base Endplates in Air

Plate Fillet Radius	Mode	Predicted Resonant Frequency	Measured Resonant Frequency	Percent Difference
1.5 inch	1T	605	596	1.5
	2B	1063	1067	-0.4
	2B,1T	1984	1825	8.7
0.75 inch	1T	586	588	-0.3
	2B	1005	1018	-1.3
	2B,1T	1920	1816	5.7
0.5 inch	1T	580	577	0.5
	2B	989	1001	-1.2
	2B,1T	1902	1789	6.3

Table 5. Comparison of Predicted and Measured Resonant Frequencies for Aluminum Plates with Base Endplates in Water

Plate Fillet Radius	Mode	Predicted Resonant Frequency	Measured Resonant Frequency	Percent Difference
1.5 inch	1T	452	472	-4.2
	2B	712	808	-11.9
	2B,1T	1523	1357	12.2
0.75 inch	1T	437	464	-5.8
	2B	670	767	-12.6
	2B,1T	1472	1315	11.9
0.5 inch	1T	432	455	-5.0
	2B	658	745	-11.7
	2B,1T	1457	1305	11.6

Table 6. The averages of the magnitude and the maximum differences between Predicted and Measured Resonant Frequencies

Averages of the Magnitude

Fluid Medium	Plate Without Base Endplates	Plate With Base Endplates
air	4.6	2.9
water	9.6	9.6

Maximum Differences

Fluid Medium	Plate Without Base Endplates	Plate With Base Endplates
air	8.4	8.7
water	17.5	12.6

A comparison of measured resonant frequencies for plates with and without base endplates is given in Tables 7 and 8 for measurements made in air and water, respectively. The measurements made with the endplates indicate that the resonant frequencies are less than those made without endplates attached. For measurements made in air, the endplates have an equivalent mass effect and decrease the resonant frequency for the first two measured modes of vibration with a maximum reduction (5.6%) occurring at the second bending mode. The third measured mode of vibration in air is less affected and its percent difference is on the order of the repeatability. Also, the percent difference appears to be independent of fillet radius except at the second bending mode of vibration. For measurements made in water, the endplates again have an equivalent mass effect but decrease the resonant frequencies for all three measured modes of vibration. This percent frequency reduction increases with frequency. In this case, the percent differences are also fillet radius independent for all modes of vibration. Figure 7 illustrates this phenomena graphically. Since the mass of the support is approximately the same as the mass of the plate, the mass ratio was calculated to be approximately one, the two structures contribute to the system frequency response, the system being the plate and the support instead of the plate only. In other words, in this study, infinite rigidity of the support can not be assumed experimentally and vibrations of the support and plate may not be occurring separately. With the addition of the endplates to the

Table 7. Comparison of Measured Resonant Frequencies for Aluminum Plates with and without Base Endplates in Air

Plate Fillet Radius	Mode	With Endplates	Without Endplates	Percent Difference
1.5 inch	1T	596	606	-1.6
	2B	1067	1128	-5.4
	2B,1T	1825	1822	0.2
0.75 inch	1T	588	597	-1.5
	2B	1018	1079	-5.6
	2B,1T	1816	1809	0.4
0.5 inch	1T	577	585	-1.4
	2B	1001	1020	-1.9
	2B,1T	1789	1777	0.7

Table 8. Comparison of Measured Resonant Frequencies for Aluminum Plates with and without Base Endplates in Water

Plate Fillet Radius	Mode	With Endplates	Without Endplates	Percent Difference
1.5 inch	1T	472	484	-2.5
	2B	808	849	-4.8
	2B,1T	1357	1444	-6.0
0.75 inch	1T	464	476	-2.5
	2B	767	811	-5.4
	2B,1T	1315	1411	-6.8
0.5 inch	1T	455	466	-2.4
	2B	745	782	-4.7
	2B,1T	1305	1393	-6.3

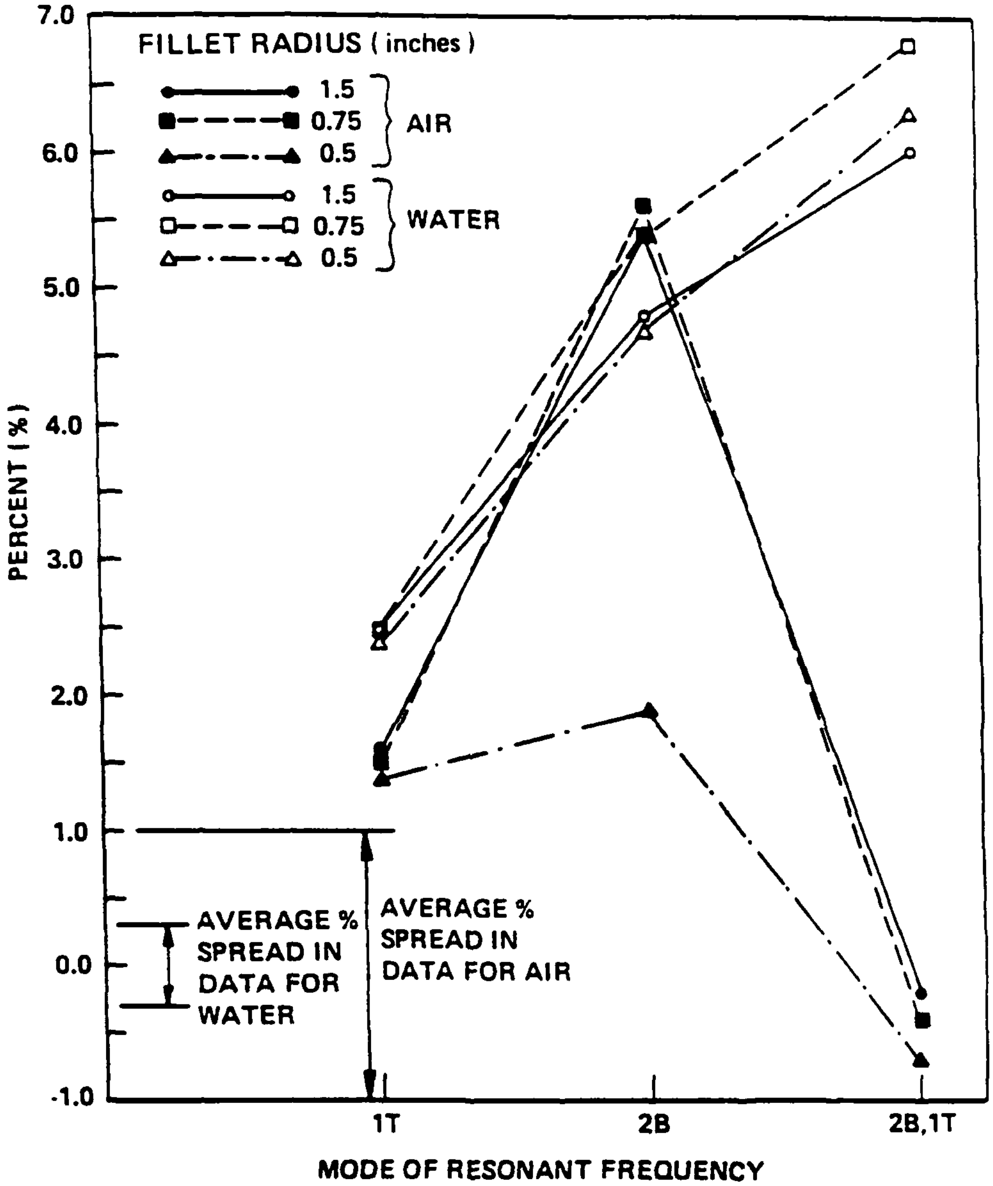

Figure 7. Percent Decrease in Measured Resonant Frequencies for Aluminum Plates Without to With Base Endplates in Air and Water

support, the entire systems' mass increases and results in reduction in resonant frequency. The attachment effects of the end plates were also investigated by simply placing the end plates in their position without bolts. The results indicate that the bolt attachment does contribute a stiffening effect by increasing the resonant frequencies. The mass effect does, however, appear to be the dominate factor for the majority of the measured values. This result gives an indication of the influence of the size of the support on the resonance frequencies.

To investigate the effects of mass numerically, the density of the support base was increased to represent a infinite mass. The results show an average increase in predicted values of 0.6 percent for the three modes of interest. The flexibility of the support was decreased, thus slightly increasing the frequencies. This indicates that numerically the base can be assumed infinitely rigid. In modeling the attachment of the endplates, various combinations of boundary conditions at the edge interface of the endplates and the plate were examined. It was found that the addition of the endplates to the model resulted in an average increase in predicted values of approximately 0.4 percent in air independent of the interface boundary condition. Based on this result, the endplate attachment scheme was made as simple as possible. The plate, endplates and support base were integrated into one unit. This model produced an average resonant frequency increase of 0.23 percent in air and 0.37 percent in water. This implies that in the finite element model the endplate attachment and connection scheme are negligible and contribute no mass effects in air or water.

Figures 8 through 13 show measured resonant frequencies versus fillet radius for each measured mode of vibration in both air and water. Each figure shows results for plates with and without base endplates attached and the average spread in data for each condition. The effects of the base endplates are clearly shown for each measured mode of vibration and fluid medium.

Figures 8 through 13 also clearly show a general trend of increasing resonant frequency with increasing plate fillet radius. Introducing a fillet reduces the effective bending length of the plate thus increasing the resonant frequencies. Also, from a theoretical analysis, Reference [5], it can be shown that a small addition of material, representing the fillet, will result in a increase in resonant frequency. The fillet region can also be viewed in terms of root flexibility. From theory, Reference [6,7], as the root flexibility decreases, i.e. as the fillet radius increases, the resonant frequency of the system increases. In general this phenomena is independent of the mode of vibration, boundary condition and fluid medium.

The effects of water loading on the reduction in the measured resonant frequencies are given in Table 9 for plates without base endplates attached and given in Table 10 for plates with base endplates attached. Tables 11 and 12 show the effects of water loading on the reduction in the predicted resonant frequencies for models without and

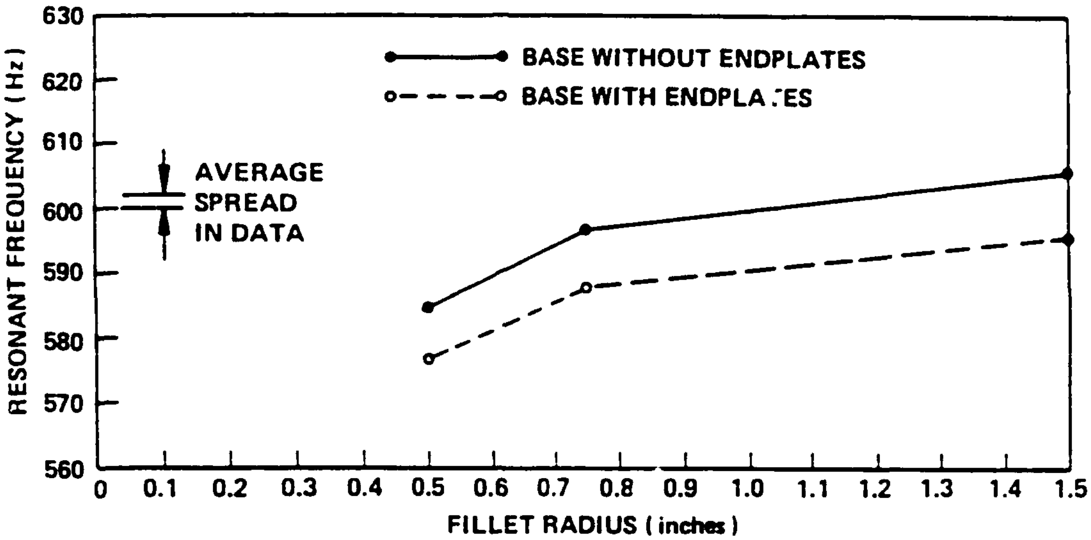

Figure 8. Measured Resonant Frequencies in Air for Plate with and without Base Endplates for First Torsional Mode (1T)

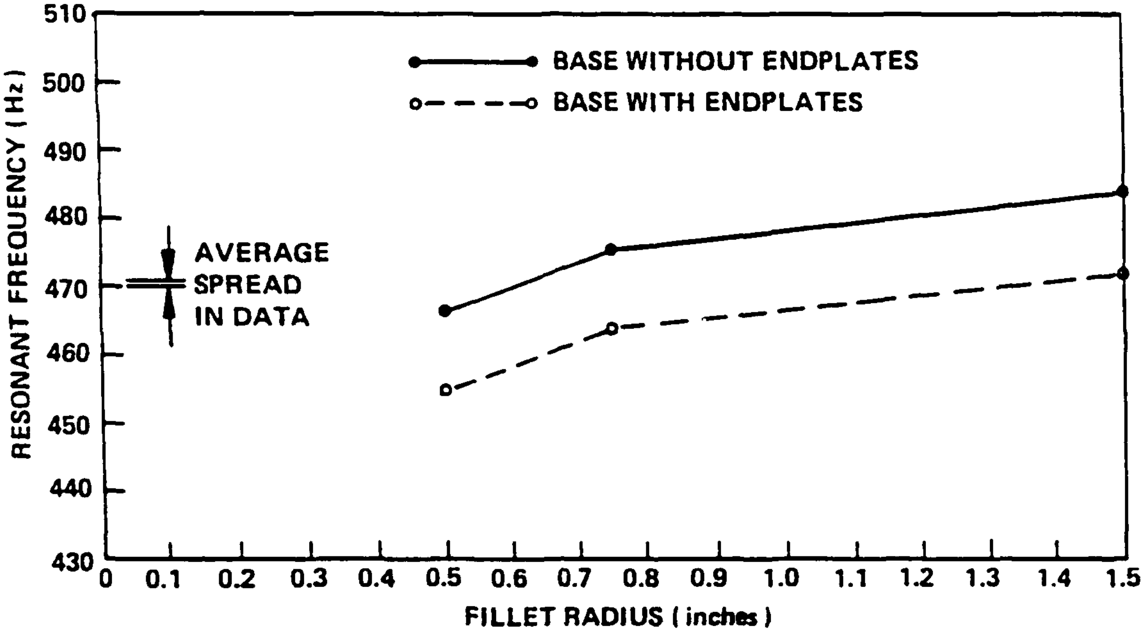

Figure 9. Measured Resonant Frequencies in Water for Plate with and without Base Endplates for First Torsional Mode (1T)

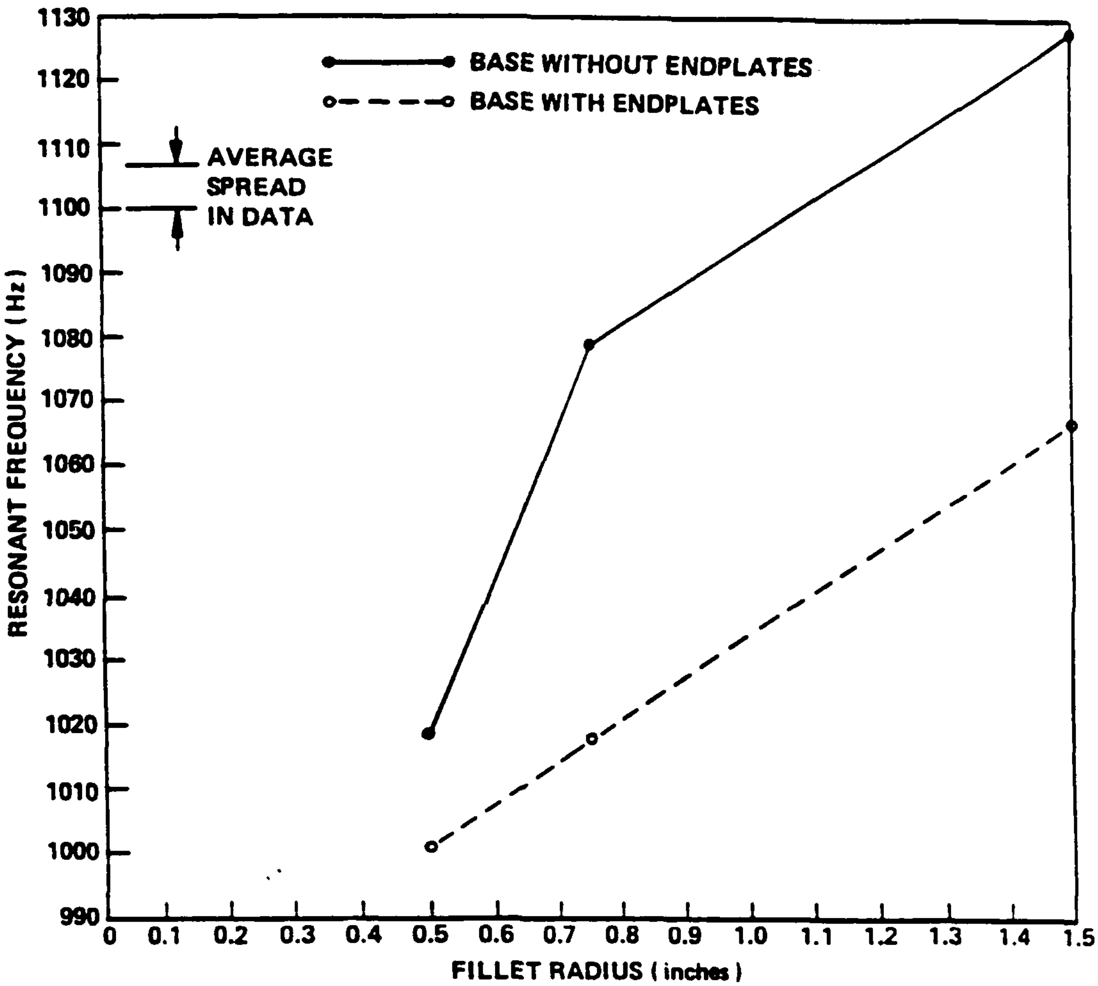

Figure 10. Measured Resonant Frequencies in Air for Plate with and without Base Endplates for Second Bending Mode (2B)

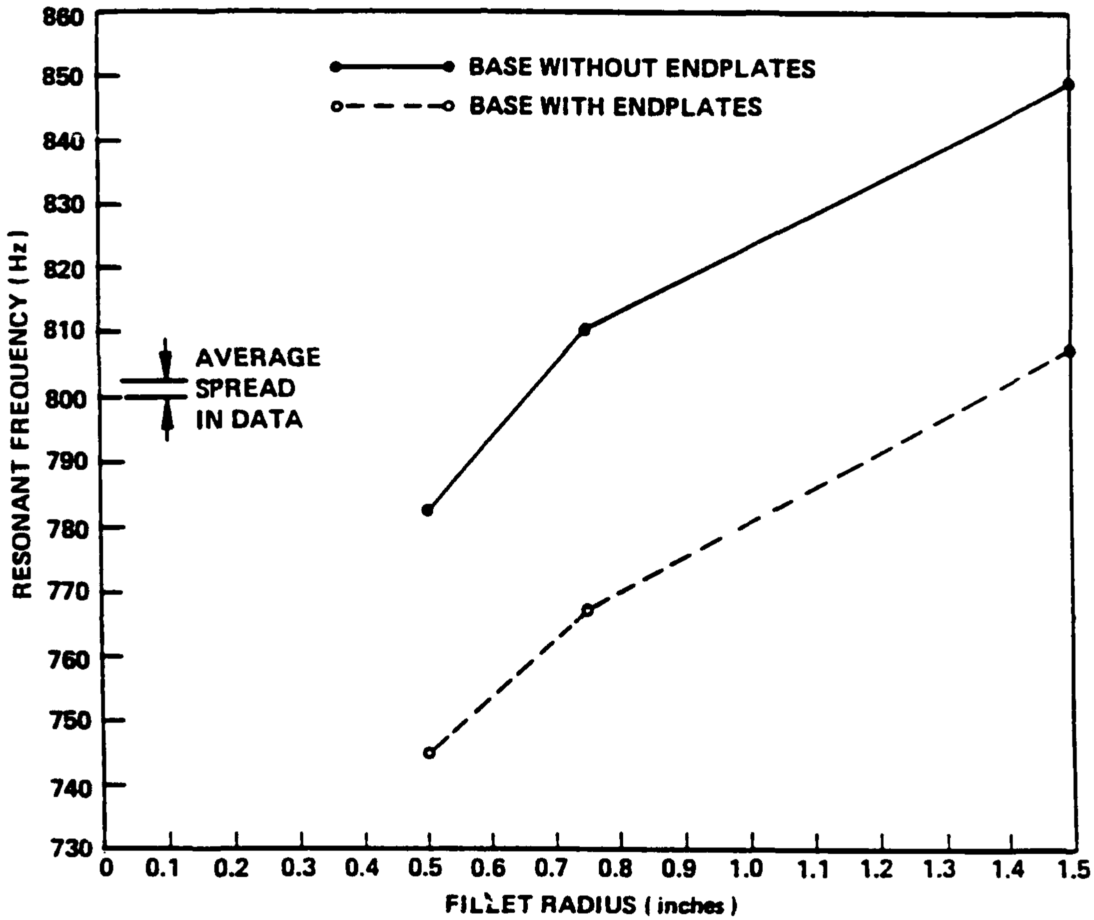

Figure 11. Measured Resonant Frequencies in Water for Plate with and without Base Endplates for Second Bending Mode (2B)

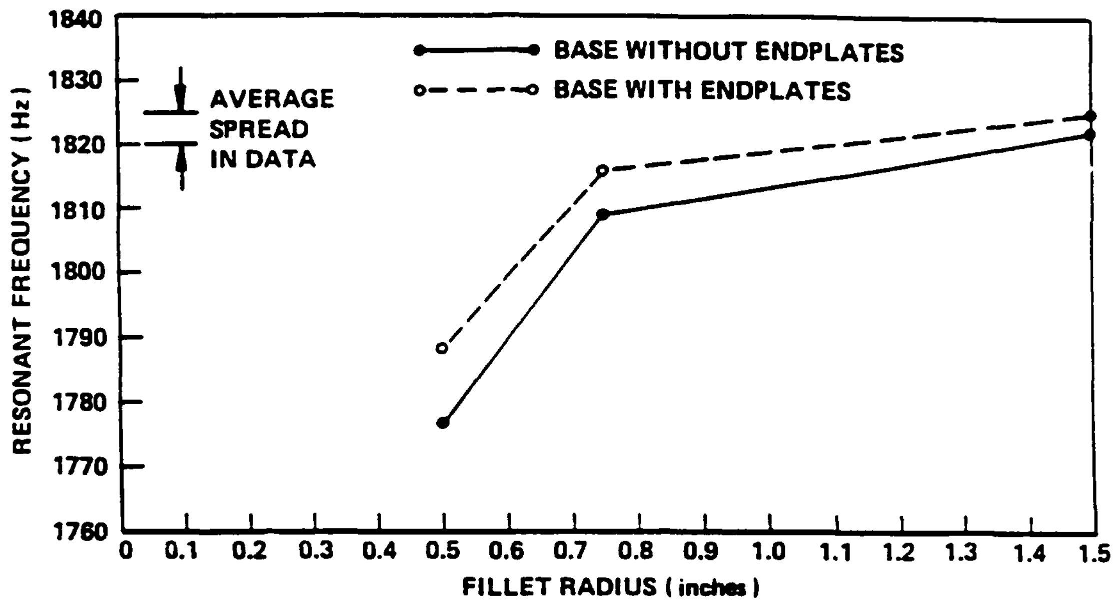

Figure 12. Measured Resonant Frequencies in Air for Plate with and without Base Endplates for Second Bending, First Torsional Mode (2B,1T)

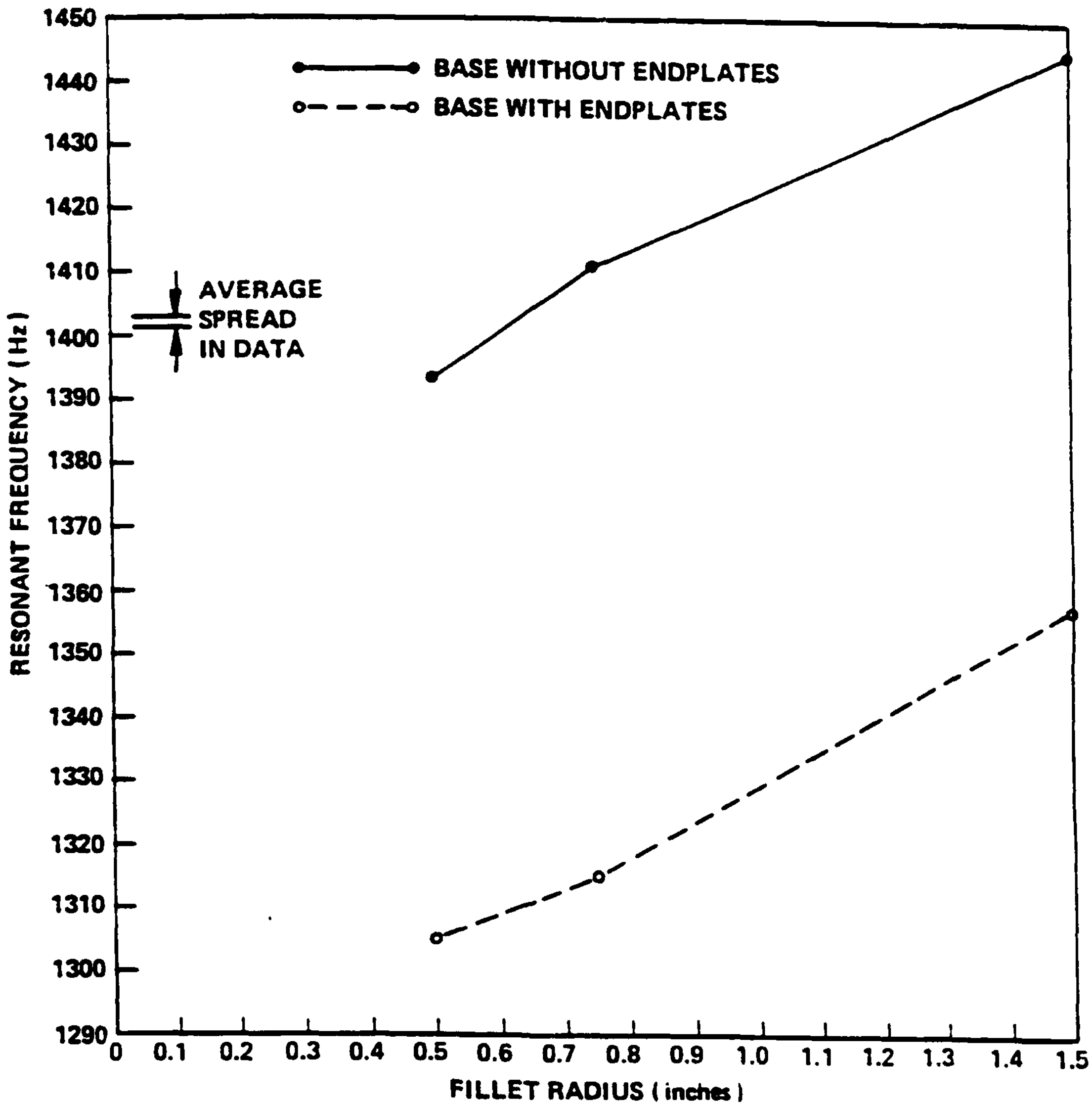

Figure 13. Measured Resonant Frequencies in Water for Plate with and without Base Endplates for Second Bending, First Torsional Mode (2B,1T)

Table 9. Resonant Frequencies Measured in Air and Water for Aluminum Plates without Base Endplates

Plate Fillet Radius	Mode	In Air	In Water	Percent Reduction
1.5 inch	1T	606	484	20
	2B	1128	849	25
	2B,1T	1822	1444	21
0.75 inch	1T	597	476	20
	2B	1079	811	25
	2B,1T	1809	1411	22
0.5 inch	1T	585	466	20
	2B	1020	782	23
	2B,1T	1777	1393	22

Table 10. Resonant Frequencies Measured in Air and Water for Aluminum Plates with Base Endplates

Plate Fillet Radius	Mode	In Air	In Water	Percent Reduction
1.5 inch	1T	596	472	21
	2B	1067	808	24
	2B,1T	1825	1357	26
0.75 inch	1T	588	464	21
	2B	1018	767	25
	2B,1T	1816	1315	27
0.5 inch	1T	577	455	21
	2B	1001	745	25
	2B,1T	1789	1305	27

Table 11. Resonant Frequencies Predicted in Air and Water for Aluminum Plates without Base Endplates

Plate Fillet Radius	Mode	In Air	In Water	Percent Reduction
1.5 inch	1T	603	449	25
	2B	1054	706	33
	2B,1T	1976	1514	23
0.75 inch	1T	585	435	26
	2B	1004	669	33
	2B,1T	1918	1467	23
0.5 inch	1T	580	431	26
	2B	988	658	33
	2B,1T	1901	1454	23

Table 12. Resonant Frequencies Predicted in Air and Water for Aluminum Plates with Base Endplates

Plate Fillet Radius	Mode	In Air	In Water	Percent Reduction
1.5 inch	1T	605	452	25
	2B	1063	712	33
	2B,1T	1984	1523	23
0.75 inch	1T	586	437	25
	2B	1005	670	33
	2B,1T	1920	1472	23
0.5 inch	1T	580	432	25
	2B	989	658	33
	2B,1T	1902	1457	23

with the base endplates attached, respectively. The effect of water loading on the reduction of the measured and predicted resonant frequencies is similar for both boundary conditions except the predicted percent reductions are much higher for the second bending mode as shown by the percentages given in the tables. For the plate without the base endplates attached, the percent reduction has a maximum at the second bending mode of vibration for the measured and predicted values. The plate with the base endplates attached shows an increase in percent reduction with increasing frequency for the measured values while the predicted values again show a maximum at the second bending mode. Figures 14 through 19 show predicted and measured resonant frequencies versus mode of vibration for each fillet radius and boundary condition. Quantitative differences between measured and predicted values are clearly shown along with resonant frequency reductions due to water loading.

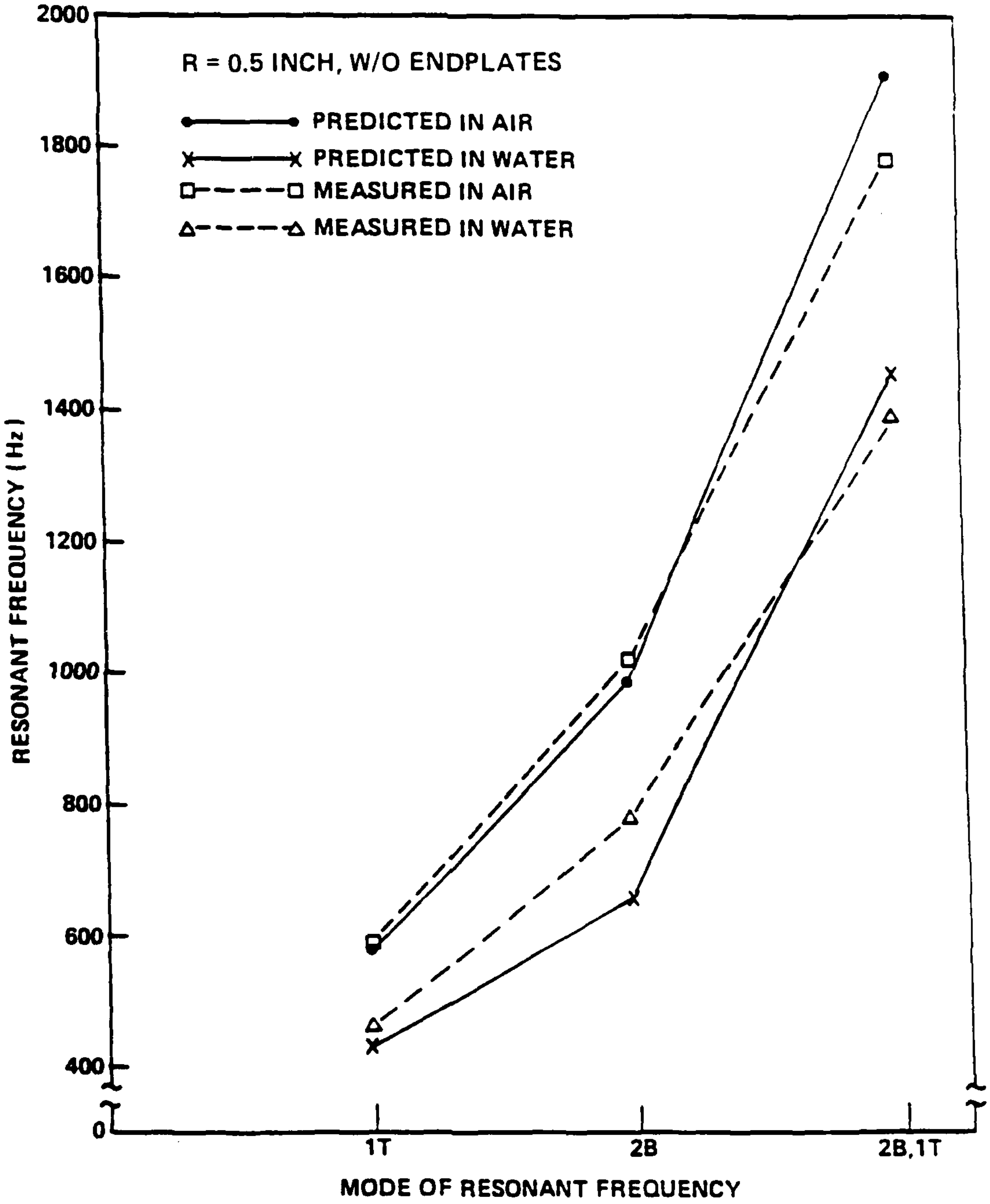

Figure 14. Predicted and Measured Resonant Frequencies in Air and Water For R = 0.5 inch without Endplates

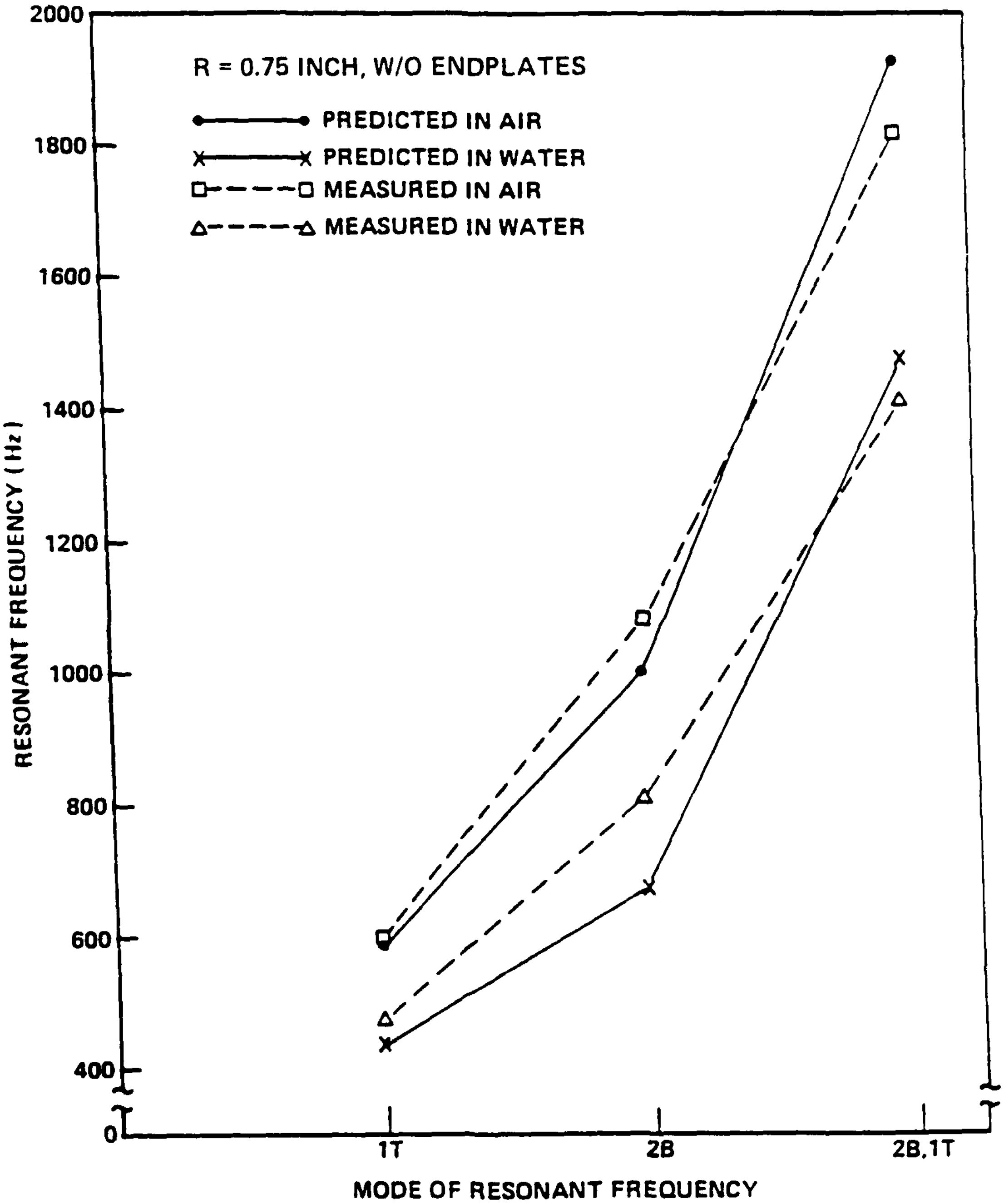

Figure 15. Predicted and Measured Resonant Frequencies in Air and Water For R = 0.75 inch without Endplates

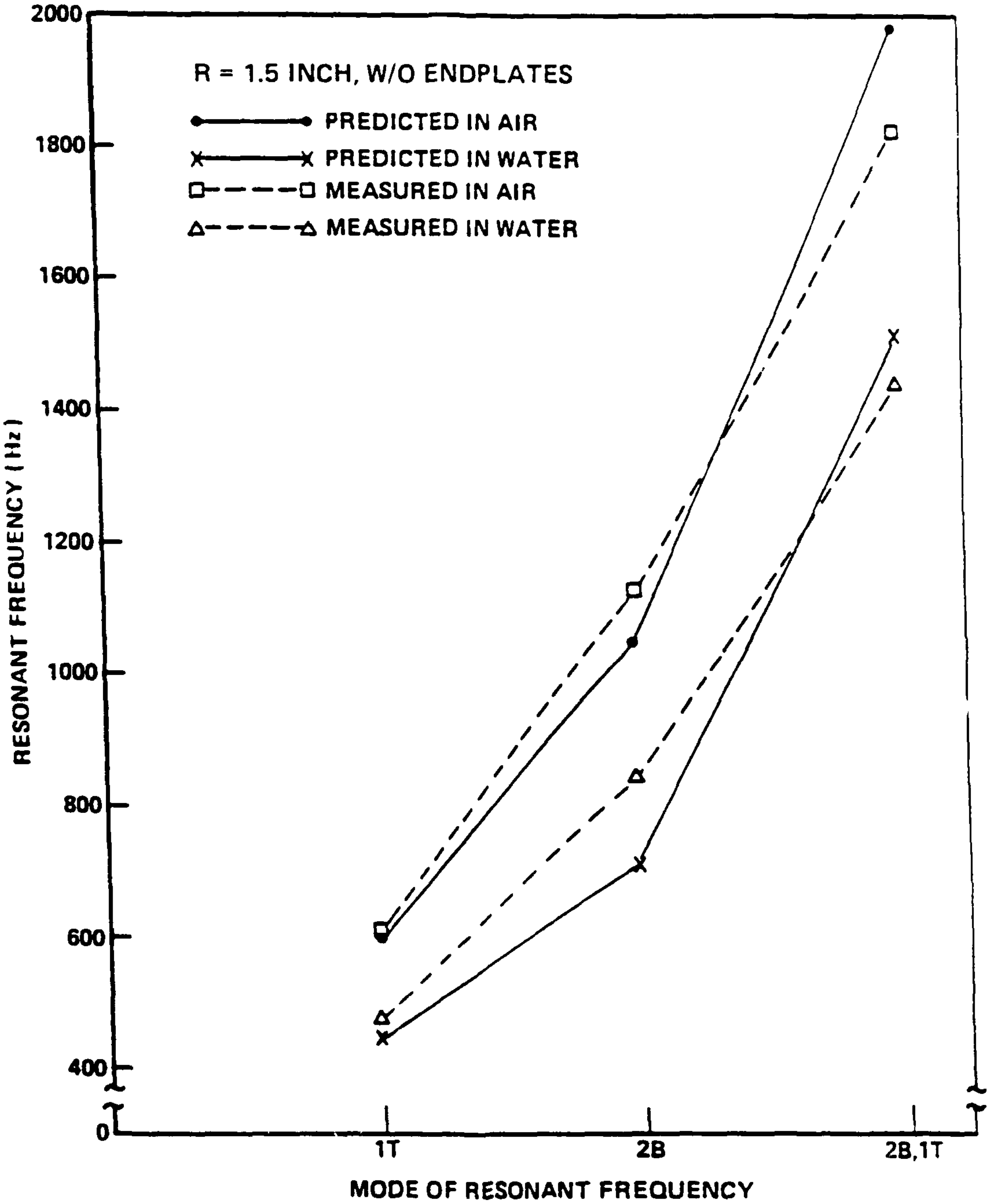

Figure 16. Predicted and Measured Resonant Frequencies in Air and Water For R = 1.5 inch without Endplates

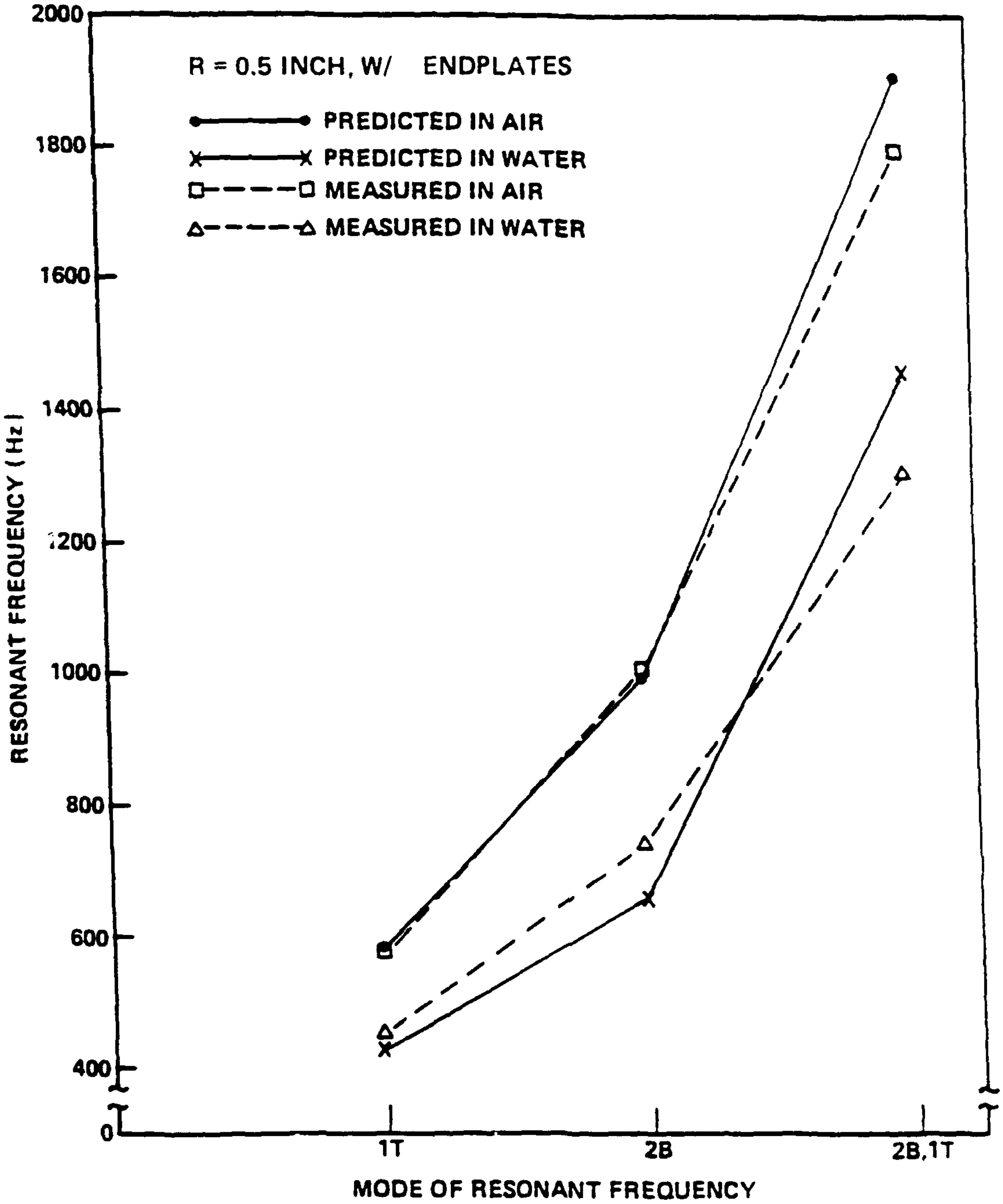

Figure 17. Predicted and Measured Resonant Frequencies in Air and Water For R = 0.5 inch with Endplates

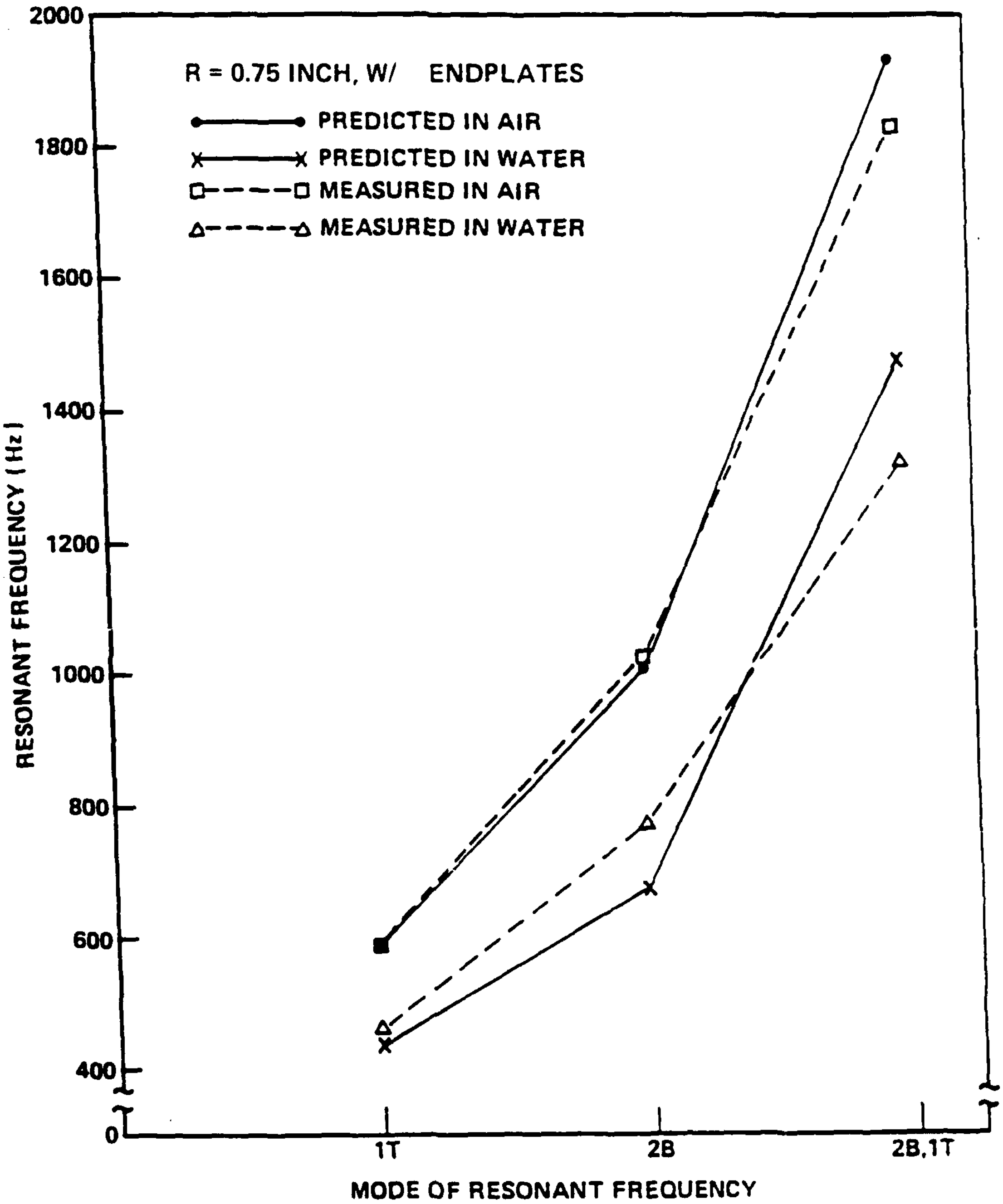

Figure 18. Predicted and Measured Resonant Frequencies in Air and Water For R = 0.75 inch with Endplates

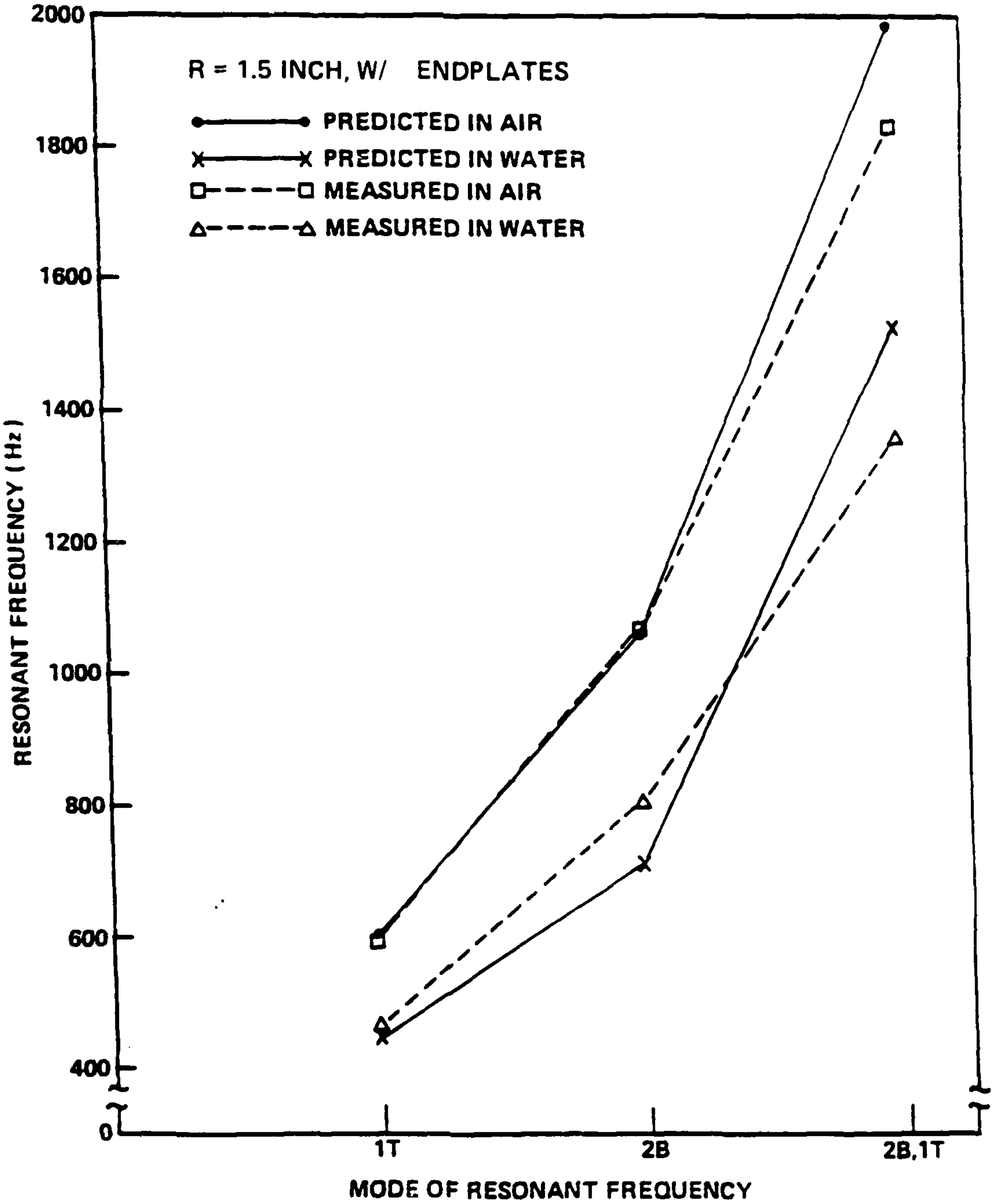

Figure 19. Predicted and Measured Resonant Frequencies in Air and Water For R = 1.5 inch with Endplates

Chapter 5

Conclusions and Recommendations for Further Research

5.1 Summary and Conclusions

The effects of certain boundary conditions, various fillet radii, and fluid media on the resonant frequencies of a flat plate fixed at one end have been quantified experimentally. A finite element model of the plate, fillet and base structure was developed. The analysis techniques used were validated against experimental results and then used to study certain effects not experimentally studied. The conclusions of the investigation are as follows:

(1) The resonant frequencies *increase as the ratio of* fillet radius *to* plate thickness increase.

(2) Specimen boundary conditions and support mass can effect resonant frequency measurements.

(3) Fluid-loading effects were shown to reduce the resonant frequencies with reductions being independent of fillet radius.

5.2 Recommendations for Further Research

In this research, measured and predicted resonant frequencies were compared for several low-order modes. Similiar studies using high-order modes would help determine the upper frequency limit of accuracy and also aide in determining the resonant frequencies boundary condition dependency at higher frequencies. The boundary conditions in numerical models should be studied in order to be able to accurately describe attachment effects and a investigation into the understanding of fluid-loading options should be done. To improve experimental measurement techniques, the effect of support mass on the resonant frequency response should be investigated. The collection of the present report along with these additional studies will aide in future experimental and numerical analysis.

References

1. C. J. D. Pickering, N. A. Halliwell, and T. H. Wilmshurst, "The Laser Doppler Vibrometer: A Portable Instrument," J. Sound Vib. 107, p.471-485 (1986).

2. R. Meynart, "A Simple Interferometric Vibrometer Based on a Laser Doppler Velocimeter," J. Phys. E 17, p.984-987 (1984).

3. P. Buchhave, "Laser Doppler Vibration Measurements Using Variable Frequency Shift," DISA Information No. 18, p.15-20 (1975).

4. MSC/NASTRAN Version 65C, MacNeal-Schwendler Corp., Los Angeles, CA (1988).

5. P. Gudmundson, "Tuning of Turbine Blades: A Theoretical Approach," J. Eng. for Power Vol. 105, p.249-255 (1983).

6. T. Justine, A. Krishnan, "Effect of Support Flexibility on Fundamental Frequency of Beams," J. Sound Vib. 68, p.310-312 (1980).

7. B. A. H. Abbas, H. Irretier, "Experimental and Theoretical Investigations of the Effect of Root Flexibility on the Vibration Characteristics of Cantilever Beams, "J. Sound Vib. 130, p.353-362 (1989).